Synthesis, spectroscopy and structure of phenylated cyclopentasilanes

Ulrich Pöschl, Harald Siegl, Karl Hassler *

Institute of Inorganic Chemistry, Graz University of Technology, Stremayrgasse 16, A-8010 Graz, Austria

Abstract

Phenylated cyclopentasilanes $Si_5Ph_{10-n}X_n$ with $X = OSO_2CF_3$, F, Cl, Br, I or H and $n = 1$ or 2 were prepared in high yield by dearylation of Si_5Ph_{10} with trifluoromethanesulphonic acid (CF_3SO_3H) and subsequent reaction with lithium or potassium halides and $LiAlH_4$. The *trans*-1,3-isomers of $Si_5Ph_8X_2$ were isolated by crystallization and the crystal structure of *trans*-1,3-difluorooctaphenyl-cyclopentasilane was determined. *cis*-1,3-, *trans*-1,2- and *cis*-1,2-$Si_5Ph_8X_2$ were identified and characterized by ^{1}H, ^{19}F and ^{29}Si NMR spectroscopy. Si–Si coupling constants were measured using INADEQUATE pulse sequences.

Keywords: Phenylated cyclopentasilanes; ^{29}Si NMR spectroscopy; Crystal structure

1. Introduction

The perphenylated cyclosilanes Si_4Ph_8, Si_5Ph_{10} and Si_6Ph_{12}, synthesized by Kipping and Sands [1] in 1921, were the first cyclosilanes to be known. Their ring structure was confirmed by Gilman and co-workers [2]. Until a few years ago, reaction with hydrogen halides was the only way to functionalize perarylated cyclosilanes. Catalytic dearylation with gaseous HCl, HBr or HI using the respective aluminium halides as catalysts allowed the preparation of the perhalogenated derivatives $(SiCl_2)_m$ [3], $(SiBr_2)_m$ [4–6] and $(SiI_2)_m$ [7] with $m = 4$, 5 or 6. In liquid HBr and HI, $Si_6Ph_6Br_6$ [5] and $Si_5Ph_5I_5$ [8], respectively, were formed. Selective mono- or disubstitution was not achieved by this kind of dearylation.

In 1979, Hengge et al. [9] synthesized the first monofunctional phenylated cyclopentasilane, Si_5Ph_9H, by means of a ring closure reaction with very low yield. Selective monofunctionalization of decaphenylcyclopentasilane was first reported by Uhlig and Tzschach [10] in 1989, namely the dearylation of Si_5Ph_{10} by use of trifluoromethanesulphonic acid (CF_3SO_3H, abbreviation TfOH, triflic acid). Among the reaction products of trifluoromethanesulphonyloxynonaphenylcyclopentasi-

lane (Si_5Ph_9OTf, nonaphenylcyclopentasilanyl triflate) with various lithium compounds, Uhlig and Tretner [11] synthesized Si_5Ph_9Cl but did not fully characterize it. Uhlig [12] also reported the introduction of a second triflate group (ditriflation) but did not determine the configuration of $Si_5Ph_8(OTf)_2$. Matyjaszewski and coworkers [13] studied the reaction of octaphenylcyclotetrasilane with triflic acid without achieving selective monosubstitution.

Our reasons for the synthesis and characterization of the phenylated cyclosilanes $Si_5Ph_{10-n}X_n$ and $Si_4Ph_{8-n}X_n$ with $X = OTf$, F, Cl, Br, I or H and $n = 1$ or 2 are the following. The stereochemistry of triflation (substitution of aryl groups by triflate groups) and subsequent exchange reactions can be studied by investigating the formation of different stereoisomers and constitutional isomers as reported in this paper. Furthermore, the partially phenylated cyclosilanes can be used for the preparation of novel, purely inorganic cyclosilanes such as $Si_5Br_8H_2$, Si_5Cl_9F and Si_4Cl_7H, and also for the synthesis of polycyclic silanes. First results concerning preparations of this kind have recently been obtained by Stüger et al. [14]. Finally, we are planning to use the synthesized compounds as targets for the study of molecular dynamics (conformational changes such as the pseudo-rotation of cyclopentasilanes and the ring flip of cyclotetrasilanes).

Our results concerning cyclotetrasilanes, particularly

---

* Corresponding author.
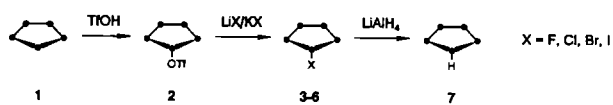
Scheme 1.
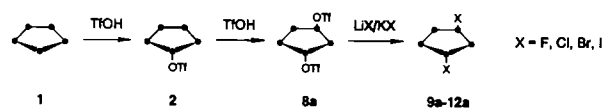
Scheme 2.

the successful monofunctionalization with triflic acid, have been summarized in Ref. [15].

2. Syntheses

Dearylation of Si_5Ph_{10} (1) using 1 equiv. of triflic acid at 0°C selectively yields Si_5Ph_9OTf (2). Further reaction of 2 with lithium or potassium halides leads to Si_5Ph_9F (3), Si_5Ph_9Cl (4), Si_5Ph_9Br (5) and Si_5Ph_9I (6), which are purified by crystallization (yield 85–95%). Si_5Ph_9H (7) is obtained by hydrogenation of any halononaphenylcyclopentasilane (3–6) with $LiAlH_4$ in over 90% yield (Scheme 1). In the reaction schemes, the dots at the edges of the five-membered cycles represent $SiPh_n$ ($n = 1$ or 2).

Ditriflation of 1 by adding a second equivalent of triflic acid to a solution of 2 at −20°C leads to trans-1,3-$Si_5Ph_8(OTf)_2$ (8a) in high yield. After reaction with lithium or potassium halides, the trans-1,3-isomers of $Si_5Ph_8F_2$ (9a), $Si_5Ph_8Cl_2$ (10a), $Si_5Ph_8Br_2$ (11a) and $Si_5Ph_8I_2$ (12a) are isolated by crystallization in 65–75% yield (Scheme 2). cis-1,3-, trans-1,2- and cis-1,2-$Si_5Ph_8X_2$ were identified as byproducts by NMR spectroscopy but could not be isolated. The spectra clearly
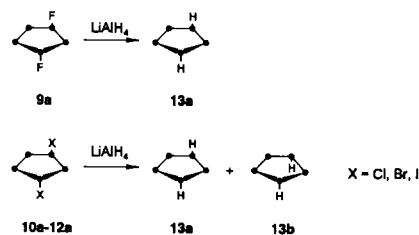
Scheme 3.

indicate the formation of trans-1,2-isomers as the dominant side reaction.

Of course, all the trans-disubstituted cyclopentasilanes exist in two enantiomeric forms, but throughout the reaction schemes only one enantiomer is shown.

Hydrogenation of trans-1,3-$Si_5Ph_8F_2$ (9a) with $LiAlH_4$ yields pure trans-1,3-$Si_5Ph_8H_2$ (13a), whereas the hydrogenation of dichloro-, dibromo- and diiodooctaphenylcyclopentasilane (10a–12a) under the same conditions leads to a mixture of 13a and cis-1,3-$Si_5Ph_8H_2$ (13b) in approximately equimolar amounts (Scheme 3).

Triflation of Si_5Ph_9F (3) at −20°C and subsequent fluorination with LiF shows another significant stereochemical aspect of the dearylation by triflic acid. Al-
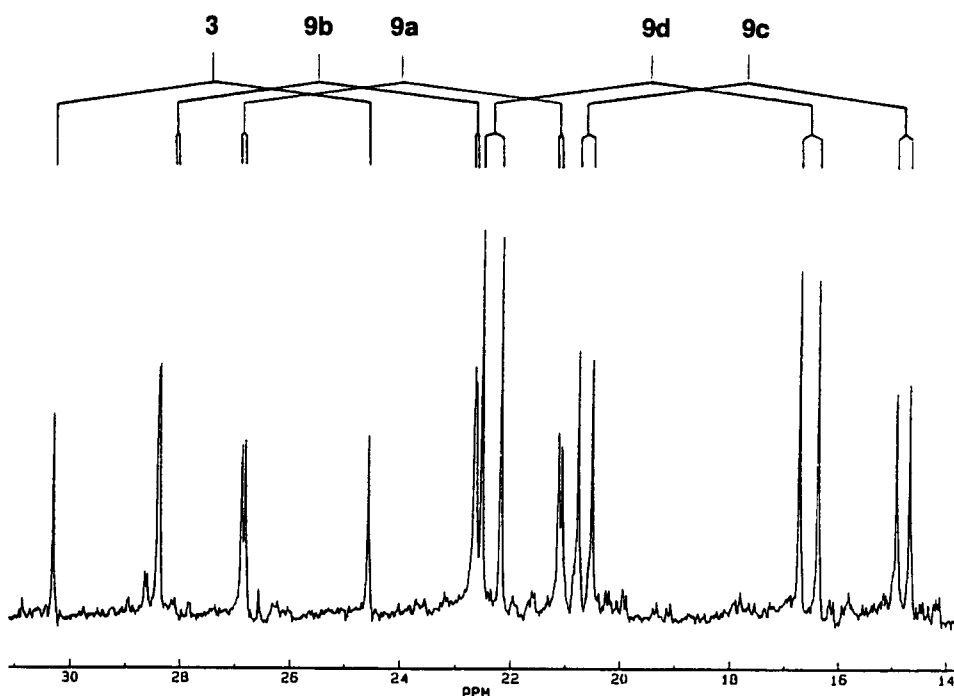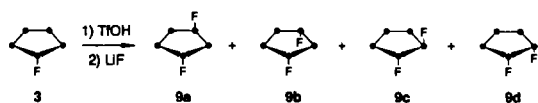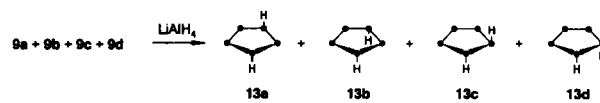

Fig. 1. ^{29}Si NMR spectrum (SiPhF region, ^1H decoupling) of an isomeric mixture of $Si_5Ph_8F_2$ (9a–d) as obtained by the reaction sequence shown in Scheme 4, with a rest of unreacted 3.

Scheme 4.

Scheme 5.

though this reaction sequence was carried out under the same conditions as the ditriflation and fluorination of 1 described above (replacing the intermediate 2 by 3), it results in the formation of all possible stereoisomers and constitutional isomers of $Si_5Ph_8F_2$ (9a–d) in practically equal amounts, except for 1,1-$Si_5Ph_8F_2$, which was not detected (Scheme 4, Fig. 1). Temperature variations between $-40°C$ and room temperature did not significantly influence the product composition.

The small stereochemical influence of the highly electronegative fluorine substituent on triflation indicates that steric effects might be more important for the high stereoselectivity of ditriflation than the strong electron-withdrawing effect of triflate groups. The same conclusion can be drawn from the observed preference

for trans-1,2- over cis-1,3-ditriflation as a side reaction of trans-1,3-ditriflation.

Hydrogenation of $Si_5Ph_8F_2$ (9a–d, as obtained from the reaction sequence shown in Scheme 4) under the usual conditions yields a mixture of 13a, 13b, trans-1,2-$Si_5Ph_8H_2$ (13c) and cis-1,2-$Si_5Ph_8H_2$ (13d) (Scheme 5).

3. NMR spectroscopy

The NMR experiments were performed in C_6D_6 at 22°C on a Bruker 300 MSL spectrometer. ^{29}Si spectra

Table 1
^{29}Si NMR data for Si_5Ph_9X (2–7)

No.	X	Si(1) δ (ppm)	Si(1) J (Hz)	Si(2, 5) δ (ppm)	Si(2, 5) J (Hz)	Si(3, 4) δ (ppm)	Si(3, 4) J (Hz)
2	OTf	33.3	^1J(Si,Si)60.4 ^2J(Si,Si)14.7	−38.9	^1J(Si,Si)60.7 ^2J(Si,Si)9.5	−34.9	^2J(Si,Si)61.0 ^2J(Si,Si)14.6 ^2J(Si,Si)9.3
3	F	27.4	^1J(Si,F)341.1 ^1J(Si,Si)66.0 ^2J(Si,Si)13.1	−41.3	^2J(Si,F)16.5 ^1J(Si,Si)65.9 ^2J(Si,Si)9.5	−34.9	^2J(Si,Si)13.1 ^2J(Si,Si)9.5
4	Cl	2.3	^1J(Si,Si)61.9 ^2J(Si,Si)13.6	−36.7	^1J(Si,Si)61.9 ^1J(Si,Si)60.9 ^2J(Si,Si)9.9	−35.0	^1J(Si,Si)60.9 ^2J(Si,Si)13.4 ^2J(Si,Si)10.0
5	Br	−5.5	^2J(Si,Si)13.8	−36.8	^1J(Si,Si)61.2 ^2J(Si,Si)10.0	−35.1	^1J(Si,Si)61.2 ^2J(Si,Si)13.7 ^2J(Si,Si)10.1
6	I	−29.4	^1J(Si,Si)55.8 ^2J(Si,Si)14.0	−37.0	^1J(Si,Si)55.9 ^2J(Si,Si)10.2	−35.0	^2J(Si,Si)14.0 ^2J(Si,Si)10.3
7	H	−60.7	^1J(Si,H)173.5	−35.3	^2J(Si,Si)10.6	−33.7	^2J(Si,Si)10.8

Table 2
^{29}Si NMR data for trans-1,3-$Si_5Ph_8X_2$ (8a–13a)

No.	X	Si(1, 3) δ (ppm)	Si(1, 3) J (Hz)	Si(2) δ (ppm)	Si(2) J (Hz)	Si(4, 5) δ (ppm)	Si(4, 5) J (Hz)
8a	OTf	28.9	^1J(Si,Si)63.1 ^2J(Si,Si)12.0	−40.7	^1J(Si,Si)63.0 ^2J(Si,Si)10.4	−39.0	^1J(Si,Si)62.8 ^2J(Si,Si)11.4
9a	F	23.8	^1J(Si,F)342.1 ^3J(Si,F)3.5 ^1J(Si,Si)66.1 ^2J(Si,Si)10.2	−46.6	^2J(Si,F)15.7 ^1J(Si,Si)65.2 ^2J(Si,Si)14.2	−40.5	^2J(Si,F)17.2 ^1J(Si,Si)66.6 ^2J(Si,Si)13.9 ^2J(Si,Si)10.3
10a	Cl	−0.5	^1J(Si,Si)62.2 ^2J(Si,Si)11.9	−38.2	^1J(Si,Si)62.0 ^2J(Si,Si)11.5	−37.2	^1J(Si,Si)63.0 ^2J(Si,Si)11.6
11a	Br	−7.8	^2J(Si,Si)12.2	−37.9	^2J(Si,Si)10.7	−37.4	^2J(Si,Si)12.2 ^2J(Si,Si)10.6
12a	I	−31.2	^1J(Si,Si)56.8 ^2J(Si,Si)12.8	−38.4	^1J(Si,Si)56.3 ^2J(Si,Si)9.8	−38.1	^1J(Si,Si)56.6 ^2J(Si,Si)12.8 ^2J(Si,Si)10.1
13a	H	−61.2	^1J(Si,H)176.1	−36.1	^2J(Si,Si)8.3	−34.0	^2J(Si,Si)8.5

Table 3
^{29}Si NMR data for trans-1,2-Si$_5$Ph$_8$X$_2$ (**9c–13c**) and cis-1,2-Si$_5$Ph$_8$X$_2$ (**9d, 13d**)

No.	X	Si(1, 2)		Si(3, 5)		Si(4)	
		δ (ppm)	J (Hz)	δ (ppm)	J (Hz)	δ (ppm)	J (Hz)
9c	F	17.7	^{1}J(Si,F)348.5 ^{2}J(Si,F)15.0	−42.4	^{2}J(Si,F)16.6 ^{3}J(Si,F)3.3	−34.3	^{3}J(Si,F)2.5
10c	Cl	−6.0	^{1}J(Si,Si)63.2 ^{2}J(Si,Si)12.5 ^{2}J(Si,Si)15.3	−36.9	^{1}J(Si,Si)63.3 ^{2}J(Si,Si)15.4	−36.2	^{2}J(Si,Si)12.4
11c	Br	−16.1	^{2}J(Si,Si)13.7	−36.5	^{2}J(Si,Si)14.3	−36.2	^{2}J(Si,Si)12.6
13c	H	−63.4	^{1}J(Si,H)181.1	−32.7		−33.1	
9d	F	19.4	^{1}J(Si,F)345.8 ^{2}J(Si,F)20.4	−41.7	^{2}J(Si,F)20.0	−34.7	^{3}J(Si,F)2.4
13d	H	−60.4	^{1}J(Si,H)176.6	−35.6		−32.4	

Table 4
^{29}Si NMR data for cis-1,3-Si$_5$Ph$_8$X$_2$ (**9b, 13b**)

No.	X	Si(1, 3)		Si(2)		Si(4, 5)	
		δ (ppm)	J (Hz)	δ (ppm)	J (Hz)	δ (ppm)	J (Hz)
9b	F	25.5	^{1}J(Si,F)343.0 ^{3}J(Si,F)1.9	−46.4	^{2}J(Si,F)18.1	−40.4	^{2}J(Si,F)17.4 ^{3}J(Si,F)1.3
13b	H	−59.8	^{1}J(Si,H)177.0	−34.7		−34.1	

were recorded at 59.6 MHz using INEPT pulse sequences [16] with ^{1}H decoupling in most cases. Experiments without polarization transfer were performed when signal intensities had to be analysed precisely. The INEPT–INADEQUATE pulse sequences [17] used for the determination of Si–Si coupling constants were optimized for ^{2}J(Si, Si), which yields the most information about the investigated substitution patterns. Unless the determination of ^{1}J(Si, Si) was possible within the same measurement, we did not determine it by additional experiments. Coupling constants are given as absolute values; the digital resolution ranges between 0.1 and 0.5 Hz. ^{19}F spectra were recorded at 282.4 MHz and ^{1}H spectra at 300.1 MHz. Chemical shifts are reported relative to TMS and CFCl$_3$, respectively.

The ^{29}Si NMR data for Si$_5$Ph$_9$X (**2–7**) and trans-1,3-Si$_5$Ph$_8$X$_2$ (**8a–13a**) are given in Tables 1 and 2. With increasing electronegativity of the halogen substituents, the signals arising from SiPhX groups show the expected increase in δ (low-field shift) [18] and an increase in ^{1}J(Si, Si) and a decrease in ^{2}J(Si, Si). For comparison, the chemical shift of Si$_5$Ph$_{10}$ (**1**) relative to TMS is −34.4 ppm.

The isomers listed in Tables 3 and 4 have not been isolated in the pure state, but by detailed analysis of Si–Si, Si–F and Si–H couplings and signal intensities it was possible to assign all their ^{29}Si signals.

For cis-1,3-Si$_5$Ph$_8$(OTf)$_2$ (**8b**) and trans-1,2-Si$_5$Ph$_8$ (OTf)$_2$ (**8c**), only the ^{29}Si signals arising from SiPhOTf groups could be assigned (δ (ppm)): **8b** Si(1, 3) 17.6; **8c** Si(1, 2) 21.8. The signals arising from the SiPh$_2$ groups of **8b** and **8c** are located at −39 ± 3 ppm and could not be assigned individually.

^{1}H NMR (δ (ppm)): Si–H: 7 5.68, **13a** 5.47, **13b** 5.39, **13c** 5.45, **13d** 5.42; phenyl-H: 7, **13a–d** 6.8–7.8.
^{19}F NMR (δ (ppm)): 3 − 191.8, **9a** − 195.2, **9b** − 194.3; **9c** − 198.2; **9d** − 197.5.

Table 5
Crystal data, data collection and refinement for **9a** grown in toluene

| Empirical formula	$C_{48}H_{40}F_2Si_5 + C_7H_8$
Formula weight (g mol^{-1})	795.27 + 92.14
Crystal system	Monoclinic
Space group	$P2/c$
a (Å)	14.655(8)
b (Å)	9.728(6)
c (Å)	33.78(2)
α (°)	90
β (°)	93.82(5)
γ (°)	90
Volume (Å^3)	4805(5)
Z	4
Temperature (K)	88(2)
Density (calcd. g cm^{-3})	1.227
Absorption coeff. (mm^{-1})	0.193
F(000)	1864
2θ range (°)	2.77–27.50
Index ranges	−19/h/18, −11/k/11, −39/l/40
Reflections collected	10109
Independent reflections	8536 (R(int) = 0.0468)
Data	8510
Parameters	560
Goodness-of-fit on F^2	1.086
Final R indices ($I > 2\sigma(I)$)	$R_1 = 0.0568$, $wR_2 = 0.1273$
R indices (all data)	$R_1 = 0.1029$, $wR_2 = 0.1647$
Largest diff. peak (e Å^{-3})	0.442
Largest diff. hole (e Å^{-3})	−0.359
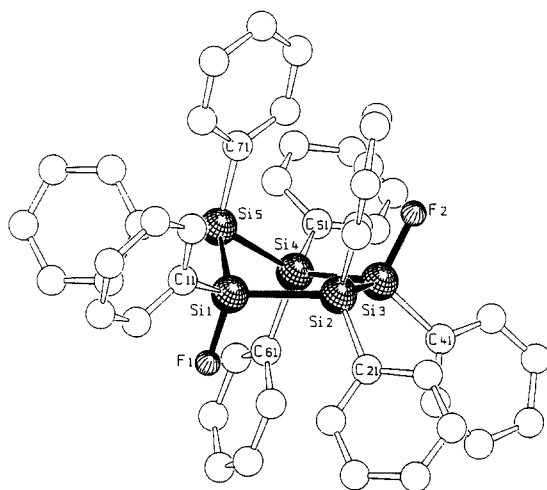
Fig. 2. Crystal structure of *trans*-1,3-Si₅Ph₈F₂ (9a). Hydrogen atoms are not shown.

4. Crystal structure of *trans*-1,3-difluorooctaphenylcyclopentasilane (9a)

Colourless single crystals of *trans*-1,3-Si₅Ph₈F₂ (9a) suitable for X-ray diffraction analysis were grown in toluene. Data collection was performed under a stream of N_2 at $-186°C$ using a modified STOE four-circle diffractometer and graphite monochromated molybdenum $K\alpha$ radiation ($\lambda = 0.71073$ Å). The crystal was mounted on the tip of a glass fibre in inert oil.

Space group $P2/c$ was chosen and later confirmed by successful structure solution. The structure was solved by direct methods using xs [19] and refined by full-matrix least squares with SHELXL-93 [20], minimizing the residuals for F^2. No absorption correction was applied. Hydrogen atoms were included in the model at their calculated positions. Anisotropic displacement pa-

Table 6
Selected intramolecular distances (Å) and angles (°) in **9a**

Si(1)–F(1)	1.629(2)	Si(3)–C(41)	1.870(4)
Si(1)–C(11)	1.871(4)	Si(3)–Si(4)	2.363(2)
Si(1)–Si(5)	2.374(2)	Si(4)–C(51)	1.884(4)
Si(1)–Si(2)	2.379(2)	Si(4)–C(61)	1.886(4)
Si(2)–C(21)	1.878(4)	Si(4)–Si(5)	2.371(2)
Si(2)–C(31)	1.886(4)	Si(5)–C(71)	1.882(4)
Si(2)–Si(3)	2.386(2)	Si(5)–C(81)	1.885(4)
Si(3)–F(2)	1.630(2)		
F(1)–Si(1)–C(11)	103.0(2)	Si(3)–Si(4)–Si(5)	101.90(6)
F(1)–Si(1)–Si(5)	106.65(9)	C(71)–Si(5)–C(81)	108.8(2)
C(11)–Si(1)–Si(5)	119.52(13)	C(71)–Si(5)–Si(4)	114.11(12)
F(1)–Si(1)–Si(2)	109.64(10)	C(81)–Si(5)–Si(4)	113.27(12)
C(11)–Si(1)–Si(2)	114.46(13)	C(71)–Si(5)–Si(1)	106.60(12)
Si(5)–Si(1)–Si(2)	103.21(6)	C(81)–Si(5)–Si(1)	115.23(13)
C(21)–Si(2)–C(31)	109.7(2)	Si(4)–Si(5)–Si(1)	98.52(6)
C(21)–Si(2)–Si(1)	113.26(14)	C(16)–C(11)–Si(1)	119.3(3)
C(31)–Si(2)–Si(1)	108.13(12)	C(12)–C(11)–Si(1)	122.7(3)
C(21)–Si(2)–Si(3)	111.12(12)	C(22)–C(21)–Si(2)	123.5(3)
C(31)–Si(2)–Si(3)	111.40(13)	C(26)–C(21)–Si(2)	120.0(3)
Si(1)–Si(2)–Si(3)	103.06(7)	C(32)–C(31)–Si(2)	119.5(3)
F(2)–Si(3)–C(41)	104.5(2)	C(36)–C(31)–Si(2)	123.4(3)
F(2)–Si(3)–Si(4)	103.92(10)	C(46)–C(41)–Si(3)	122.3(3)
C(41)–Si(3)–Si(4)	115.02(13)	C(42)–C(41)–Si(3)	119.7(3)
F(2)–Si(3)–Si(2)	109.82(9)	C(56)–C(51)–Si(4)	122.2(3)
C(41)–Si(3)–Si(2)	116.27(13)	C(52)–C(51)–Si(4)	120.7(3)
Si(4)–Si(3)–Si(2)	106.52(7)	C(66)–C(61)–Si(4)	121.3(3)
C(51)–Si(4)–C(61)	110.1(2)	C(62)–C(61)–Si(4)	121.9(3)
C(51)–Si(4)–Si(3)	109.52(13)	C(76)–C(71)–Si(5)	123.9(3)
C(61)–Si(4)–Si(3)	111.96(12)	C(72)–C(71)–Si(5)	118.5(3)
C(51)–Si(4)–Si(5)	115.01(12)	C(82)–C(81)–Si(5)	122.2(3)
C(61)–Si(4)–Si(5)	108.12(11)	C(86)–C(81)–Si(5)	120.4(3)

Table 7
Selected torsion angles (°) in **9a**

Si(5)–Si(1)–Si(2)–Si(3)	−31.13(6)	C(31)–Si(2)–C(21)–C(22)	128.0(5)
Si(1)–Si(2)–Si(3)–Si(4)	0.70(6)	C(21)–Si(2)–C(31)–C(32)	−34.8(4)
Si(2)–Si(3)–Si(4)–Si(5)	29.85(7)	C(61)–Si(4)–C(51)–C(52)	−85.5(3)
Si(3)–Si(4)–Si(5)–Si(1)	−48.09(7)	C(51)–Si(4)–C(61)–C(62)	152.3(3)
Si(2)–Si(1)–Si(5)–Si(4)	49.42(6)	C(81)–Si(5)–C(71)–C(72)	65.0(3)
F(1)–Si(1)–C(11)–C(12)	172.0(3)	C(71)–Si(5)–C(81)–C(82)	16.1(3)
F(2)–Si(3)–C(41)–C(42)	−17.3(4)		

Table 8
Fractional atomic coordinates (10^{-4}) and equivalent isotropic displacement parameters $(10^{-3} \, \text{Å}^2)$ of the non-hydrogen atoms of the asymmetric unit containing 9a and toluene, C(1)–C(7)

Atom	x	y	z	U_{eq} [a]
Si(1)	7079(1)	951(1)	6669(1)	22(1)
Si(2)	8498(1)	2095(1)	6610(1)	23(1)
Si(3)	8489(1)	2578(1)	5917(1)	23(1)
Si(4)	7089(1)	1725(1)	5628(1)	22(1)
Si(5)	6112(1)	1959(1)	6156(1)	21(1)
F(1)	7183(1)	−666(2)	6554(1)	30(1)
F(2)	8421(2)	4232(2)	5844(1)	34(1)
C(11)	6694(2)	881(4)	7185(1)	29(1)
C(12)	6625(3)	2055(5)	7422(1)	41(1)
C(13)	6336(3)	1935(7)	7806(1)	59(2)
C(14)	6112(3)	672(8)	7958(1)	71(2)
C(15)	6177(3)	−485(7)	7730(1)	63(2)
C(16)	6467(3)	−386(5)	7346(1)	43(1)
C(21)	9515(2)	1022(4)	6779(1)	28(1)
C(22)	9457(3)	−339(6)	6883(2)	86(2)
C(23)	10240(4)	−1090(7)	7005(3)	137(4)
C(24)	11080(4)	−454(6)	7024(2)	74(2)
C(25)	11151(3)	862(5)	6914(1)	50(1)
C(26)	10380(3)	1589(5)	6798(1)	43(1)
C(31)	8489(2)	3726(4)	6912(1)	29(1)
C(32)	8799(3)	3697(5)	7310(1)	44(1)
C(33)	8733(4)	4848(6)	7552(1)	63(2)
C(34)	8359(4)	6037(6)	7401(2)	62(2)
C(35)	8055(3)	6108(5)	7006(2)	50(1)
C(36)	8122(3)	4961(4)	6765(1)	38(1)
C(41)	9528(2)	2039(4)	5664(1)	30(1)
C(42)	9886(3)	2904(6)	5386(1)	50(1)
C(43)	10630(3)	2534(7)	5179(2)	63(2)
C(44)	11033(3)	1262(6)	5248(1)	57(1)
C(45)	10697(3)	378(5)	5524(1)	51(1)
C(46)	9947(3)	780(5)	5735(1)	41(1)
C(51)	6740(3)	2752(4)	5170(1)	26(1)
C(52)	7390(3)	3200(4)	4918(1)	37(1)
C(53)	7148(4)	3980(5)	4581(1)	48(1)
C(54)	6254(4)	4310(4)	4493(1)	50(1)
C(55)	5595(4)	3874(6)	4733(1)	56(1)
C(56)	5842(3)	3115(5)	5073(1)	46(1)
C(61)	7162(2)	−158(4)	5501(1)	24(1)
C(62)	7748(2)	−1058(4)	5720(1)	27(1)
C(63)	7784(3)	−2451(4)	5632(1)	33(1)
C(64)	7234(3)	−2981(4)	5323(1)	39(1)
C(65)	6651(3)	−2132(4)	5103(1)	39(1)
C(66)	6610(3)	−732(4)	5190(1)	32(1)
C(71)	5916(2)	3790(4)	6309(1)	23(1)
C(72)	5506(3)	4029(4)	6664(1)	32(1)
C(73)	5344(3)	5362(4)	6796(1)	39(1)
C(74)	5583(3)	6478(4)	6568(1)	39(1)
C(75)	5993(3)	6264(4)	6219(1)	37(1)
C(76)	6152(2)	4928(4)	6089(1)	29(1)
C(81)	4970(2)	1093(4)	6056(1)	24(1)
C(82)	4162(3)	1831(4)	6000(1)	34(1)
C(83)	3326(3)	1174(5)	5918(1)	42(1)
C(84)	3295(3)	−234(5)	5895(1)	49(1)
C(85)	4090(3)	−990(5)	5949(2)	59(1)
C(86)	4914(3)	−335(4)	6025(1)	42(1)
C(1)	11084(4)	−3859(7)	6226(2)	69(2)
C(2)	11257(5)	−5288(7)	6229(2)	81(2)
C(3)	12124(5)	−5747(7)	6379(2)	78(2)
C(4)	12678(5)	−4849(10)	6503(2)	90(2)
C(5)	12618(5)	−3529(9)	6490(2)	84(2)
C(6)	11793(4)	−3030(6)	6359(2)	77(2)
C(7)	10178(5)	−3319(11)	6066(3)	164(5)

[a] U_{eq} is defined as one third of the trace of the orthogonalized U_{ij} tensor.

rameters were assigned to all non-hydrogen atoms and isotropic displacement parameters were used for hydrogen atoms. A summary of crystal data, data collection and refinement is given in Table 5.

The centrosymmetric space group $P2/c$ is characterized by a twofold rotation axis perpendicular to a mirror plane. Accordingly, the unit cell comprises both enantiomers of *trans*-1,3-Si$_5$Ph$_8$F$_2$. Along with two molecules of each enantiomer, the cell contains four molecules of toluene.

The structure of 9a is shown in Fig. 2. Selected intramolecular angles, distances and torsion angles are summarized in Tables 6 and 7. The estimated standard deviations in parentheses refer to the last digit. Fractional coordinates and equivalent isotropic thermal parameters for the asymmetric unit containing 9a and toluene are given in Table 8.

A comparison of the crystal structures of *trans*-1,3-Si$_5$Ph$_8$F$_2$ (9a, grown in toluene) and Si$_5$Ph$_{10}$ (1, grown in benzene, monoclinic, space group $C/2c$, $Z = 8$ [21]) shows some significant differences. In 9a the silicon ring adopts an envelope conformation with approximate C_s symmetry (torsion angles 49.4, −31.1, 0.7, 29.8, −48.1°), whereas the silicon ring in 1 is puckered in a form intermediate between C_s and C_2 symmetry (torsion angles 41.9, −30.2, 7.3, 18.4, −37.0°). The Si–Si–Si angles in 9a range from 98.5 to 106.5° and in 1 from 102.7 to 106.7°. The Si–Si bond lengths vary between 2.363 and 2.386 Å in 9a and between 2.371 and 2.413 Å in 1. The average Si–C distance in 9a is 1.880 Å and in 1 it is 1.895 Å.

Distances of 1.630(2) and 1.629(2) Å were determined for the Si–F bonds in 9a. To our knowledge, these are the largest Si–F bond lengths that have been measured for oligosilanes, exceeding the Si–F bond length in Si$_2$H$_5$F, 1.598(8) Å, which was determined by microwave spectroscopy [22].

Detailed crystallographic data for 9a have been deposited at the Cambridge Crystallographic Data Centre, Cambridge, UK.

5. Experimental details

5.1. Techniques

All operations with triflate or halogen compounds were carried out under a nitrogen atmosphere. Triflate and iodine compounds are highly sensitive to moisture. In contrast, the fluorine, chlorine and bromine derivatives are stable for several hours when exposed to air. Solvents were distilled from potassium. Lithium and potassium halides were dried by heating for several

hours in vacuo. Trifluoromethanesulphonic acid was used as received from Merck–Schuchardt (Art. 821166) (1.71 g cm^{-3}, 98%). Si$_5$Ph$_{10}$ (1) was prepared by ring closure of SiPh$_2$Cl$_2$ with lithium according to [7].

Paraffinic suspensions held between CsBr plates were used to record IR spectra on a Perkin-Elmer Model 883 infrared spectrophotometer. Melting points were determined with a Büchi 530 apparatus and are uncorrected.

C,H analyses were carried out on a Heraeus Mikro U apparatus (tolerances: ±0.3% C, ±0.2% H). Of all compounds, only the measured carbon content of non-aphenylcyclopentasilane fell below the tolerance. Despite the addition of PbBO$_3$ for complete fusion, this deviation was presumably due to incomplete oxidation (formation of silicon carbide).

5.2. Synthesis of Si$_5$Ph$_9$X (2–7)

Compound 1 (9.50 g, 10.4 mmol) was dissolved in toluene (300 ml) and cooled to 0°C. Within 10 min triflic acid (98%, 1.00 ml, 11.2 mmol) was added dropwise. Then the ice-bath was removed and the reaction mixture was stirred at room temperature for 20 h, until all the suspended triflic acid had been consumed. By evaporation in vacuo the solution of 2 was reduced to ca. 70 ml. For the synthesis of 3, 4 and 5 diethyl ether (70 ml) and LiF (0.4 g, 15 mmol), LiCl (0.6 g) or LiBr (1.3 g) were added at 0°C. For 6, 1,2-dimethoxyethane (70 ml) and KI (2.5 g) were used instead. The resulting suspension was stirred at room temperature for 6 h, then the solvents were removed in vacuo. Toluene (60 ml) was added and the salts were removed by filtration at 50°C. Crystallization from toluene–heptane yields the pure halononaphenylcyclopentasilanes (3–6) as colourless crystals (yield 85–95%).

For the synthesis of 7, any halononaphenylcyclopentasilane (3–6, 10 mmol) was dissolved in a mixture of toluene (60 ml) and diethyl ether (60 ml) and LiAlH$_4$ (5 mmol dissolved in 2.5 ml of diethyl ether) was added dropwise at 0°C. The reaction mixture was stirred at room temperature for 20 h, then was slowly poured into 1 M H$_2$SO$_4$ (100 ml) at 0°C. After double extraction with diethyl ether (2 × 60 ml), the organic phase was dried over sodium sulphate and filtered. The solvents were removed in vacuo and the residue was crystallized from a mixture of ethyl acetate and heptane, yielding nonaphenylcyclopentasilane (7) as a microcrystalline white powder (yield > 90%).

Fluorononaphenylcyclopentasilane (3): 853.38 g mol^{-1}; m.p. 88–92°C; anal. C$_{54}$H$_{45}$FSi$_5$ (exp./calc.), C 75.73 / 76.00, H 5.39 / 5.32%; IR (< 1000 cm^{-1}), 997m, 971w, 915vw, 887vw, 850w, 798m, 733vs, 725sh, 695vs, 685sh, 670sh, 618vw, 552vw, 516vw, 473vs, 420vw, 377vw, 355sh, 343s, 327s, 305vw.

Chlorononaphenylcyclopentasilane (4): 869.83 g mol^{-1}; m.p. 112–114°C; anal. C$_{54}$H$_{45}$ClSi$_5$(exp./calc.), C 74.63/74.56, H 5.37/5.21%; IR (< 1000 cm^{-1}), 997m, 971vw, 916vw, 851w, 745w, 732vs, 693vs, 683sh, 668vw, 620vw, 538m, 521w, 488w, 481vw, 475s, 467w, 459m, 446w, 437sh, 419m, 381vw, 370w, 357vw, 342s, 322s, 302vw, 295w.

Bromononaphenylcyclopentasilane (5): 914.28 g mol^{-1}; m.p. > 250°C; anal. C$_{54}$H$_{45}$BrSi$_5$ (exp./calc.); C 70.92/70.94%, H 5.10/4.96%; IR (< 1000 cm^{-1}), 997m, 970vw, 916vw, 852w, 733vs, 694vs, 680sh, 619vw, 535vw, 518w, 474vs, 468sh, 460sh, 450sh, 435sh, 418s, 370sh, 365m, 360sh, 340s, 322s, 294w.

Iodononaphenylcyclopentasilane (6): 961.28 g mol^{-1}; m.p. > 250°C; anal. C$_{54}$H$_{45}$ISi$_5$ (exp./calc.), C 67.21/67.47, H 4.91/4.72%; IR (< 1000 cm^{-1}), 997m, 969vw, 915vw, 849w, 732vs, 695vs, 680sh, 619vw, 532vw, 513w, 475vs, 465sh, 452sh, 435sh, 417m, 405sh, 356m, 334s, 322s, 292w.

Nonaphenylcyclopentasilane (7): 835.38 g mol^{-1}; m.p. 115–119°C; anal. C$_{54}$H$_{46}$Si$_5$ (exp./calc.), C 77.30/77.64, H 5.54/5.43%; IR (< 1000 cm^{-1}, except for ν(SiH)), 2080m, 996m, 915w, 847m, 800vw, 775m, 733vs, 722sh, 695vs, 682sh, 668sh, 618w, 548w, 530sh, 515sh, 507m, 475vs, 450sh, 417w, 373w, 335sh, 327s, 300vw.

5.3. Synthesis of trans-1,3-Si$_5$Ph$_8$X$_2$ (8a–13a)

Compound 1 (9.50 g, 10.4 mmol) was dissolved in toluene (300 ml) and cooled to 0°C. Within 10 min, triflic acid (1.00 ml, 11.2 mmol) was added dropwise, then the ice-bath was removed and the reaction mixture was stirred at room temperature for 20 h, until all the suspended triflic acid had been consumed. At −20°C the second portion of triflic acid (1.00 ml, 11.2 mmol) was added. After 4 h at −20°C and 4 h at 0°C, the reaction mixture was stirred at room temperature for another 15 h. By evaporation in vacuo the solution of 8a was reduced to ca. 70 ml. For the synthesis of 9a, 10a and 11a, diethyl ether (70 ml) and LiF (0.8 g, 30 mmol), LiCl (1.3 g) or LiBr (2.6 g) were added at 0°C. For 12a, 1,2-dimethoxyethane (70 ml) and KI (5.0 g) were used instead. The resulting suspension was stirred at room temperature for 6 h, then the solvents were removed in vacuo. Toluene (60 ml) was added and the salts were removed by filtration at 50°C. Crystallization from toluene–heptane yielded the trans-1,3-dihalooctaphenylcyclopentasilanes (9a–12a) as colourless crystals (yield 65–75%).

For the synthesis of 13a, trans-1,3-Si$_5$Ph$_8$F$_2$ (9a, 7.95 g, 10 mmol) was dissolved in a mixture of toluene (60 ml) and diethyl ether (60 ml) and LiAlH$_4$ (10 mmol dissolved in 5 ml of diethyl ether) was added dropwise at 0°C. The reaction mixture was stirred at room temperature and after 20 h it was slowly poured into 1 M

H_2SO_4 (100 ml) at 0°C. After double extraction with diethyl ether (2 × 60 ml), the organic phase was dried over sodium sulphate and filtered. The solvents were removed in vacuo and crystallization from toluene–heptane yielded *trans*-1,3-dihydrooctaaphenylcyclopentasilane (**13a**) as colourless crystals (yield 90–95%).

trans-1,3-Difluorooctaphenylcyclopentasilane (**9a**): 795.27 g mol^{-1}; m.p. 125–130°C (decomp.); anal. $C_{48}H_{40}F_2Si_5$ (exp./calc.), C 72.21/72.49, H 5.25/5.07%; IR (< 1000 cm^{-1}), 996m, 970w, 932vw, 917w, 890vw, 854w, 802s, 792s, 735vs, 695vs, 675sh, 617vw, 545vw, 520w, 471vs, 460s, 450s, 425sh, 385w, 340s, 331s, 290w.

trans-1,3-Dichlorooctaphenylcyclopentasilane (**10a**): 828.18 g mol^{-1}; m.p. 216–220°C; anal. $C_{48}H_{40}Cl_2Si_5$ (exp./calc.), C 69.53/69.61, H 5.04/4.87%; IR (< 1000 cm^{-1}), 997m, 971vw, 915vw, 854w, 736vs, 696vs, 688sh, 618w, 602vw, 545m, 539sh, 519vw, 490s, 475s, 464m, 455s, 443sh, 425vw, 375w, 357w, 338s, 330s, 312vw, 280w.

trans-1,3-Dibromooctaphenylcyclopentasilane (**11a**): 917.08 g mol^{-1}; m.p. 215–225°C; anal. $C_{48}H_{40}Br_2Si_5$ (exp./calc.), C 62.63/62.87, H 4.42/4.40%; IR (< 1000 cm^{-1}), 997m, 973w, 919vw, 847w, 735vs, 694vs, 618vw, 535vw, 527vw, 517w, 472vs, 463s, 454m, 437m, 417s, 365m, 332vs, 330sh, 291w.

trans-1,3-Diiodooctaphenylcyclopentasilane (**12a**): 1011.08 g mol^{-1}; m.p. 240–244°C; anal. $C_{48}H_{40}I_2Si_5$ (exp./calc.), C 57.25/57.02, H 4.15/3.99%; IR (< 1000 cm^{-1}), 997m, 970vw, 916vw, 849w, 734vs, 694vs, 618vs, 535m, 518w, 503vw, 467s, 462sh, 448m, 421w, 401m, 394sh, 362sh, 367vw, 346vw, 322s, 314s, 288w.

trans-1,3-Dihydrooctaphenylcyclopentasilane (**13a**): 759.29 g mol^{-1}; m.p. 159–164°C; anal. $C_{48}H_{42}Si_5$ (exp./calc.), C 75.81/75.93, H 5.68/5.58%; IR (< 1000 cm^{-1}, except for ν(SiH)), 2100s, 996m, 973vw, 916w, 854w, 772s, 778s, 735vs, 696vs, 672s, 617vw, 536m, 512sh, 508m, 470vs, 455w, 447w, 434vw, 419vw, 381w, 348s, 312w, 302sh, 294w.

References

[1] F.S. Kipping and H.E. Sands, *J. Chem. Soc., 119* (1921) 830, 848.

[2] A. Jarvie, H.S. Winkler, D.J. Peterson and H. Gilman, *J. Am. Chem. Soc., 83* (1961) 1921; H. Gilman and G. Schwabke, *J. Am. Chem. Soc., 86* (1964) 2693; Th. Kinstle, I. Haiduc and H. Gilman, *Inorg. Chim. Acta, 3* (1969) 373.

[3] E. Hengge and D. Kovar, *J. Organomet. Chem., 125* (1977) C29; *Z. Anorg. Allg. Chem., 458* (1979) 163.

[4] E. Hengge and G. Bauer, *Angew. Chem., 85* (1973) 304; *Monatsh Chem., 106* (1975) 503.

[5] E. Hengge and F. Lunzer, *Monatsh. Chem., 107* (1976) 371.

[6] D. Kovar, K. Utvary and E. Hengge, *Monatsh Chem., 110* (1979) 1295.

[7] E. Hengge and D. Kovar, *Angew. Chem., 93* (1981) 698.

[8] E. Hengge and H. Marketz, *Monatsh Chem., 100* (1969) 890.

[9] E. Hengge, D. Kovar und H.P. Söllradl, *Monatsh. Chem., 110* (1979) 805.

[10] W. Uhlig and A. Tzschach, *J. Organomet. Chem., 378* (1989) C1.

[11] W. Uhlig and C. Tretner, *J. Organomet. Chem., 436* (1992) C1.

[12] W. Uhlig, *Chem. Ber., 125* (1992) 47.

[13] J. Chruściel, M. Cypryk, E. Fossum and K. Matyjaszewski, *Organometallics, 11* (1992) 3257.

[14] H. Stüger, P. Lassacher and E. Hengge, *J. Organomet. Chem.*, submitted for publication.

[15] U. Pöschl and K. Hassler, *Organometallics*, in press.

[16] G.A. Morris and R. Freeman, *J. Am. Chem. Soc., 101* (1979) 760.

[17] O.W. Sorensen, R. Freeman, T. Frenkiel and R. Schuck, *J. Magn. Reson., 46* (1982) 180.

[18] H. Marsmann, in P. Diehl, E. Fluck and R. Kosfeld (eds.), *NMR Basic Principles and Progress*, Vol. 17, Springer, Berlin, 1981.

[19] SHELXTL 4.1, Siemens Crystallographic Research System, 1990.

[20] G.M. Sheldrick, SHELXL-93, University of Göttingen, 1993.

[21] L. Parkanyi, K. Sasvari, J.P. Declercq and G. Germain, *Acta Crystallogr., Sect. B, 34* (1978) 3678.

[22] A.P. Cox and R. Varma, *J. Chem. Phys., 44* (1966) 2619.